European Journal of Medicinal Chemistry 45 (2010) 4788–4796

Contents lists available at ScienceDirect

European Journal of Medicinal Chemistry

journal homepage: http://www.elsevier.com/locate/ejmech

Original article

Synthesis and evaluation of novel stearoyl-CoA desaturase 1 inhibitors: 1′-{6-[5-(pyridin-3-ylmethyl)-1,3,4-oxadiazol-2-yl]pyridazin-3-yl}-3,4-dihydrospiro[chromene-2,4′-piperidine] analogs

Yoshikazu Uto [a,*], Yuko Ueno [a], Yohei Kiyotsuka [a], Yuriko Miyazawa [b], Hitoshi Kurata [a], Tsuneaki Ogata [c], Makiko Yamada [d], Tsuneo Deguchi [d], Masahiro Konishi [e], Toshiyuki Takagi [b], Satoko Wakimoto [e], Jun Ohsumi [e]

[a] Lead Discovery & Optimization Research Laboratories I, Daiichi Sankyo Co., Ltd., 1-2-58 Hiromachi, Shinagawa-ku, Tokyo 140-8710, Japan
[b] Clinical Development Department I, Daiichi Sankyo Co., Ltd., 1-2-58 Hiromachi, Shinagawa-ku, Tokyo 140-8710, Japan
[c] Global Project Management Department, Daiichi Sankyo Co., Ltd., 1-2-58 Hiromachi, Shinagawa-ku, Tokyo 140-8710, Japan
[d] Drug Metabolism & Pharmacokinetics Research Laboratories Daiichi Sankyo Co., Ltd., 1-2-58 Hiromachi, Shinagawa-ku, Tokyo 140-8710, Japan
[e] Cardiovascular-Metabolics Research Laboratories, Daiichi Sankyo Co., Ltd., 1-2-58 Hiromachi, Shinagawa-ku, Tokyo 140-8710, Japan

ARTICLE INFO

Article history:
Received 9 June 2010
Received in revised form
16 July 2010
Accepted 24 July 2010
Available online 4 August 2010

Keywords:
SCD1 inhibitor
Spiropiperidine
Oxadiazole

ABSTRACT

In continuation of our investigation on novel stearoyl-CoA desaturase (SCD) 1 inhibitors, we have already reported on the structural modification of the benzoylpiperidines that led to a series of novel and highly potent spiropiperidine-based SCD1 inhibitors. In this report, we would like to extend the scope of our previous investigation and disclose details of the synthesis, SAR, ADME, PK, and pharmacological evaluation of the spiropiperidines with high potency for SCD1 inhibition. Our current efforts have culminated in the identification of 5-fluoro-1′-{6-[5-(pyridin-3-ylmethyl)-1,3,4-oxadiazol-2-yl]pyridazin-3-yl}-3,4-dihydrospiro[chromene-2,4′-piperidine] (**10e**), which demonstrated a very strong potency for liver SCD1 inhibition ($ID_{50} = 0.6$ mg/kg). This highly efficacious inhibition is presumed to be the result of a combination of strong enzymatic inhibitory activity (IC_{50} (mouse) = 2 nM) and good oral bioavailability ($F > 95\%$). Pharmacological evaluation of **10e** has demonstrated potent, dose-dependent reduction of the plasma desaturation index in C57BL/6J mice on a high carbohydrate diet after a 7-day oral administration (q.d.). In addition, it did not cause any noticeable skin abnormalities up to the highest dose (10 mg/kg).

1. Introduction

Stearoyl-CoA desaturase 1 (SCD1) is a rate-limiting enzyme in the biosynthesis of monounsaturated fatty acids from their saturated fatty acid precursors [1–3]. SCD1 is located in the membrane of the endoplasmic reticulum (ER) and introduces a double bond at the Δ9 position (between carbons 9 and 10) of stearoyl (C18:0) and palmitoyl-CoA (C16:0) [1–3] in conjunction with NAD(P)H, cytochrome b5 reductase, and cytochrome b5. The products of SCD1, oleic (C18:1 $n-9$) and palmitoleic acids (C16:1 $n-7$) are the most abundant fatty acids found in phospholipids, cholesterol esters, and triglycerides. There are four isoforms (SCD1-4) [4] in the mouse genome and two in the human genome (1 and 5) [5]. The human SCD1 gene shows 85% homology to murine SCD1 [6].

SCD1 has recently been shown to be a crucial factor in lipid metabolism and body weight control [7–10]. In adult mice, the SCD1 isoform is expressed in lipogenic tissues including the liver and adipose tissue. Deficiency of SCD1 has been shown to cause defective hepatic cholesterol ester and triglyceride synthesis [7], resistance against obesity [8,9], and reduced liver steatosis in rodents [10]. In humans, a higher desaturation index (the ratio of oleate to stearate or 18:1/18:0) is strongly correlated with higher plasma triglyceride levels and (to a lesser extent) with plasma HDL levels [11]. The 18:1/18:0 ratio in plasma VLDL has recently been shown to be closely associated with the hepatic SCD1 expression in humans [12]. Even though the detailed mechanism by which SCD1 deficiency affects body weight and adiposity is not completely understood, inhibition of SCD1 may represent a novel approach for the treatment of metabolic syndrome.

Since Xenon Pharmaceuticals published the first example of small molecule SCD1 inhibitors (**1**, Fig. 1) in 2005 [13], numerous structures of SCD1 inhibitors have been reported in patents and

* Corresponding author. Tel.: +81 3 3492 3131; fax: +81 3 5436 8563.
E-mail address: uto.yoshikazu.pw@daiichisankyo.co.jp (Y. Uto).

0223-5234/$ – see front matter © 2010 Elsevier Masson SAS. All rights reserved.
doi:10.1016/j.ejmech.2010.07.044

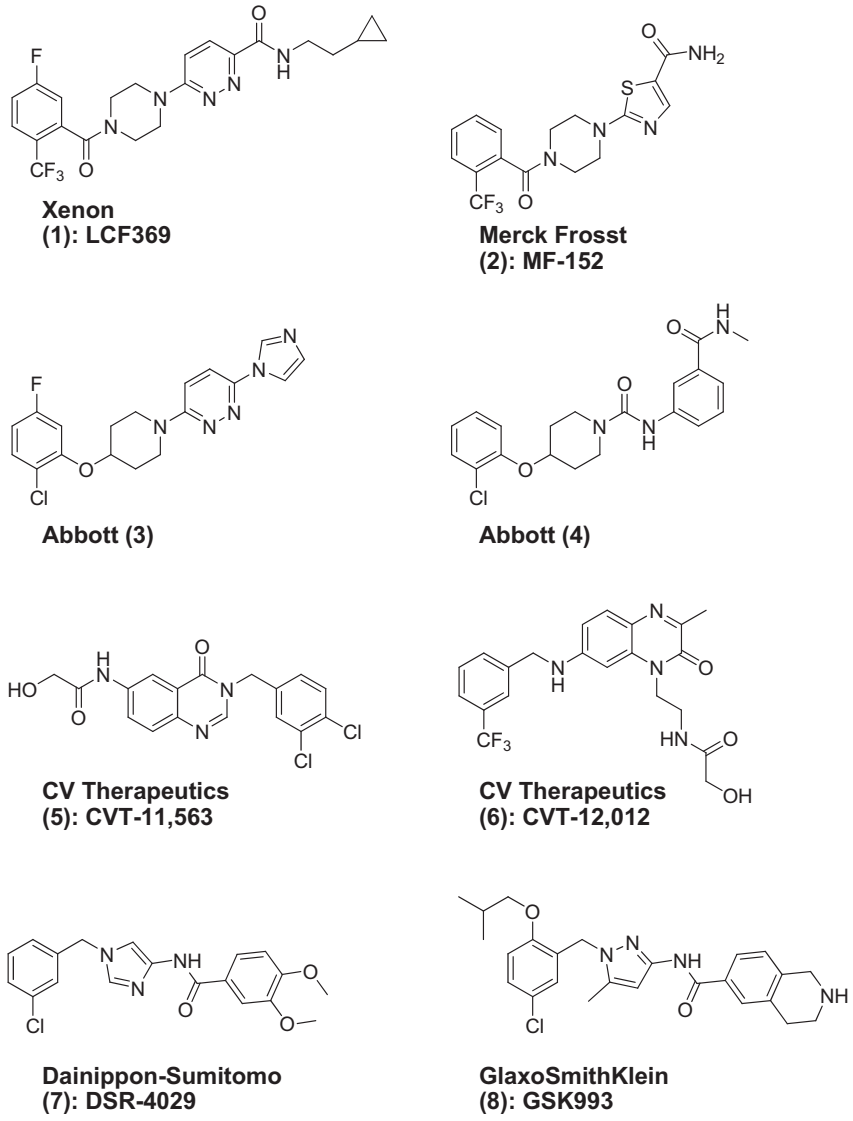

Fig. 1. Structures of small molecule-based SCD1 inhibitors.

scientific literature [14,15]. For example, Merck Frosst [16–18] and Abbott Laboratories [19–21] described a series of piperazine- or phenoxypiperidine-based SCD1 inhibitors (**2**, **3**, and **4**, Fig. 1). CV Therapeutics (Gilead) reported 2-oxo-2*H*-quinoxalin-based structures [22] and subsequently disclosed the structures of CVT-11,563 (**5**) [23] and CVT-12,012 (**6**) [24]. A class of aminoimidazole analogs, represented by DSR-4029 (**7**) [25], was revealed by Dainippon-Sumitomo. In addition, GlaxoSmithKlein recently demonstrated that the pyrazole-based inhibitor GSK993 (**8**) exerted a considerable reduction in hepatic lipids as well as a significant improvement of glucose tolerance in Zucker fatty rats [26]. We also previously reported 3-(2-hydroxyethoxy)-*N*-(5-benzylthiazol-2-yl) benzamides as potent SCD1 inhibitors [27,28].

Previously, we reported on the optimization of benzoylpiperidine-based SCD1 inhibitors (**9**) [29] and subsequent structural exploration, which successfully culminated in the discovery of highly potent spiropiperidine-based SCD1 inhibitors such as (**10c**, Fig. 2) [30]. We would like to extend the scope of our previous investigation in this report and disclose the synthesis and structure–activity relationship (SAR), as well the details of our optimization effort with respect to absorption distribution metabolism excretion (ADME) and pharmacokinetic (PK) properties. We are also disclosing the details of our in vivo pharmacological evaluation (Fig. 2).

2. Chemistry

The SCD1 inhibitors exhibited in Tables 1–4 were prepared in accordance with the procedures that were briefly described in our previous reports [29,30]. The condensation reactions of the *o*-hydroxyacetophenones (**11**) with *N*-protected 4-oxopiperidine to form spiropiperidine structures (**12**) and subsequent functional group manipulation are outlined in Scheme 1. The starting materials, properly substituted *o*-hydroxyacetophenones, were either purchased (**11e**–**f**) or prepared (**11a**–**d**) by multi-step synthesis as described previously [30]. (See Supplementary data for the experimental procedures.) The condensation reaction proceeded in alcoholic solvent and was mediated by pyrrolidine, which is the most commonly used secondary amine for this type of reaction [31,32]. The functional group manipulation on the spiropiperidines was carried out in accordance with the procedures described previously [30]. Most of the spiropiperidines (except Cl-substituted **12a**) were subjected to the same sequence of reactions (reduction of ketone, mesylation, elimination to

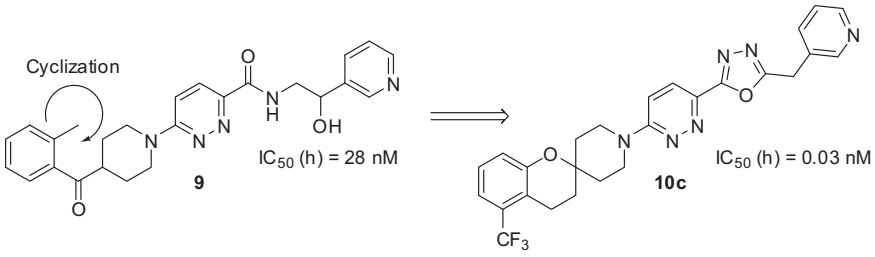

Fig. 2. Optimization of piperidine-based SCD1 inhibitors.

provide **14b**–**f**, hydrogenation under acidic conditions, and if necessary, acidic Boc-deprotection) to provide **13b**–**f** without complication for a good overall yield. In the case of **13a**, with an aim to prevent losing Cl in hydrogenation, the hydroxyl group was removed by triethylsilane and $BF_3 \cdot Et_2O$ in 95% yield. The ethylcarbamate, used instead of Boc in order to overcome the acidic reductive conditions, was hydrolyzed with KOH in aqueous EtOH solution at 100 °C to provide **13a** in 95% yield.

Preparation of the chloropyridazine intermediates and the final condensation between the spiropiperidines and the chloropyridazines are shown in Scheme 2. It was important to maintain a temperature below 55 °C in the chlorination of commercially available **15**. Above that temperature, over-chlorination occurred and desired product **16** was contaminated with over-chlorinated impurities that could only be separated with difficulty after repetitive chromatography. Hydrazides **18**, prepared from the corresponding esters (**17**), were condensed with freshly prepared **16**. Subsequent cyclization of the diacylhydrazide intermediates on the reactive chloropyridazines to provide the 1,3,4-oxadiazoles (**19**) was so problematic that initial attempts employing mild conditions such as $PPh_3/C_2Cl_6/Et_3N$ [33] or $TsCl/Et_3N$ [34] were disappointing as they produced complex mixtures. After careful optimization of the reaction conditions, a combination of TsCl and DMAP in CH_3CN provided the desired oxadiazole in good yield (62% for **19a**). The amide derivative (**21**) was prepared from amine (**20**) and **16** by the analogous procedures described for **19**. The final coupling reaction between the spiropiperidines (**13a**–**f**) and the chloropyridazines (**19a**–**c**, **21**) proceeded without complication in n-BuOH with heating to provide the desired SCD1 inhibitors.

3. Results and discussion

In Table 1, SAR studies of the right-hand pyridyl portion of the spiropiperidine-based SCD1 inhibitors are summarized. The inhibitory activity was measured for all compounds against both mouse and human SCD1. Mouse liver microsomes were used as a source of murine SCD1 while microsome fractions prepared from 293A cells were used as a source of human SCD1. While other isoforms of SCD are known to exist in mouse liver, their expression levels are low. In cellular assay, whole transfected 293A cells were used for the evaluation of our SCD1 inhibitors. It is of note that there are some differences in SAR results of the right-hand pyridyl portion in Table 1 from those of the previous investigation of the benzoylpiperidine template [29]. In the benzoylpiperidines series, 3-pyridyl analog exhibited distinctly stronger inhibitory activity against human SCD1 in the cellular assay than 2-pyridyl or 4-pyridyl analog. The 3-pyridyl analog showed 9-fold or 3-fold increased inhibitory activity compared to the 2-pyridyl or the 4-pyridyl analogs, respectively [29]. On the other hand, in this spiropiperidine series, all three pyridyl analogs (regardless of the position of the nitrogen) showed comparable inhibitory activity against human SCD1 in the cellular assay. The inhibitory activity of these compounds against SCD1 in vivo was determined and compared by measuring the ratio of [^{14}C] stearate and [^{14}C] oleate in the liver of db/db mice. ID_{50} is defined as dose at which 50% of the conversion was achieved. While the difference in the inhibitory activity against enzymatic murine SCD1 of the 3 different pyridyl derivatives was almost negligible, 3-pyridyl analog (**10f**) showed 3-fold increased potency in SCD inhibition in the liver (ID_{50}) compared to 2-pyridyl (**22**) or 4-pyridyl (**23**) after oral administration to db/db mice. The role of 1,3,4-oxadiazole moiety as an effective amide replacement was evaluated by comparing SCD1 inhibitory activity of **10f** to that of **24**. As shown in Table 1, **10f** exhibited stronger inhibitory activity across the board than amide congener **24**.

As a result of SAR studies summarized in Table 1, the right-hand portion was set as 3-pyridyl-1,3,4-oxadiazole, and the left-hand spiropiperidine portion was then investigated. As exemplified in Table 2, the available positions for substitution on the phenyl were numbered as 5, 6, 7, and 8. In our previous study [30], we indicated

Table 1
Evaluation of the right-hand portion.[a]

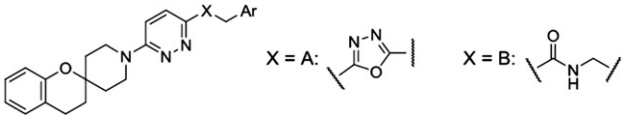

Compd	X	Ar	Enzymatic assay[b]		Cellular assay[b]	Liver desaturase inhibition[b] ID_{50} (mg/kg)
			IC_{50}[b] (nM)	IC_{50} (nM)	IC_{50} (nM)	
			Mouse microsomal Δ9	Human cell (293A) microsomal Δ9	Human cell (293A) Δ9	
22	A	2-Pyridyl	3	4	9	6
10f	A	3-Pyridyl	2	1	4	2
23	A	4-Pyridyl	4	6	7	7
24	B	3-Pyridyl	10	27	76	5

[a] Values are the arithmetic means of at least two experiments.
[b] See Experimental for the procedures for the desaturase assay, cellular assay and the determination of ID_{50}.

Table 2
Evaluation of the substituents on the spiropiperidine system.[a]

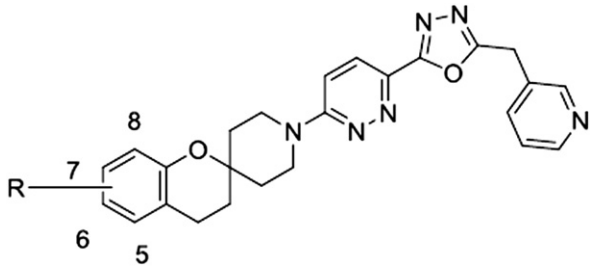

Compd	R	Enzymatic assay[b]		Cellular assay[b]	Liver desaturase inhibition[b] ID_{50} (mg/kg)
		IC_{50}[b] (nM)	IC_{50} (nM)	IC_{50} (nM)	
		Mouse microsomal Δ9	Human cell (293A) microsomal Δ9	Human cell (293A) Δ9	
10a	5-Cl	0.04	0.06	1	1
10b	5,8-Di-F	0.5	0.1	1	<2[c]
10c	5-CF_3	0.06	0.03	0.8	0.4
10d	5-Me	0.2	0.2	0.7	1
10e	5-F	2	0.3	0.7	0.6
10f	H	2	1	4	2

[a] Values are the arithmetic means of at least two experiments.
[b] See Experimental for the procedures for the desaturase assay, cellular assay and the determination of ID_{50}.
[c] 71% inhibition at 2 mg/kg.

that 6- or 7-substituted analogs showed only marginal inhibitory activity, so in the current work only 5- and 5,8-disubstituted analogs were prepared and evaluated. As anticipated from our previous investigation [30] on the spiropiperidines with pyridazine-3-carboxamide, 5-halo, 5-haloalkyl, 5-alkyl, and 5,8-dihalo analogs demonstrated strong inhibitory activity in all the assays measured in this study, namely the enzymatic inhibition of both murine and human SCD1, cellular SCD1 (human), and liver desaturation inhibition in db/db mice. The CF_3 analog was clearly the most potent one in the previous investigation [30] on the spiropiperidines with pyridazine-3-carboxamide. However, in this investigation on the [5-(pyridin-3-ylmethyl)-1,3,4-oxadiazol-2-yl] pyridazine series, the 5-fluoro analog (**10e**) exhibited comparable inhibitory activity in cellular assay and liver desaturase inhibition in db/db mice to the 5-CF_3 analog (**10c**). It is interesting that **10e** demonstrated as much potency in the liver desaturase assay as **10c** even though **10e** showed weaker inhibitory activity against enzymatic SCD1. We assume that this is because the hepatic concentration of **10e** in the db/db mice is higher than that of **10c**. Due to easier access to the key intermediate in its synthesis, **10e** is now considered as an attractive alternative to **10c**, which was elaborately prepared and established in the previous report [30] as an extremely potent SCD1 inhibitor (For detailed synthetic procedures for the preparation of the key intermediate **11c**, see Supplementary data.).

In Table 3, ADME and pharmacokinetic (PK) properties of the 5-substituted spiropiperidines are summarized. The 5,8-disubsituted analog was not investigated because access to the spiropiperidines with this substitution is rather limited, and the potency of the compound (**10b**) was not superior to the simpler 5-mono substituted congeners. The spiropiperidines (**10a**,**c**–**f**) are generally soluble in acidic aqueous media (JP-1: pH = 1.2) presumably due to the presence of basic nitrogen atoms. On the other hand, they are marginally soluble in neutral aqueous media (JP-2: pH = 6.8). The lipophilicity, expressed as calculated log *P* (*c* log *P*), of this class of compounds is between 1.7 and 2.9 and is well in the range of the value recommended in the Lipinski's rule of 5 (*c* log *P* <5) [35]. While no significant difference was observed in solubility and lipophilicity, there was a remarkable difference in PK properties in C57BL/6J mice after oral administration among the 5-

Table 3
ADME and pharmacokinetic profiles[a] of spiropiperidine-based SCD1 inhibitors.

No.	Solubility[b]			PK[d] (po, 20 mg/kg)			
	JP-1 (pH = 1.2) (μM)	JP-2 (pH = 6.8) (μM)	*c* log *P*[c]	C_{max} (μg/mL)	T_{max} (h)	$t_{1/2}$ (h)	AUC $_{(0-8\ h)}$(μg h/mL)
10a	>50	<0.5	2.6	0.69	0.8	0.7	1.4
10c	88	<0.5	2.9	2.6	1.0	1.4	7.8
10d	91	<0.5	2.2	1.1	0.8	0.6	2.1
10e	>100	<0.5	2.0	2.9	1.3	1.0	6.8
10f	92	4.2	1.7	1.3	1.0	0.8	2.4

[a] Values are the arithmetic means of at least two experiments.
[b] Aqueous acidic (JP-1) and neutral solution (JP-2) were purchased from Kanto Chemical Co., Inc. The sample solution was assayed using HPLC methodologies. 250 μM of the compound solution in aqueous CH_3CN solution (1:1 (v/v)) was prepared to make a calibration curve. The solubility was determined by comparing the UV peak area of the standard solution.
[c] The *c* log *P* values were calculated by CLOGP software (Version 4.8.2, Daylight Chemical Information Systems, Inc.).
[d] A dose of each compound was orally (20 mg/kg, PG/Tween = 4:1, *n* = 3) administered using an intubation tube. Plasma samples (20 μL) were collected up to 8 h after intravenous or oral administration.

Table 4
Summary of ADME.[a]

ADME			PK[e]		
c log *P*[b]		2.0	(iv) 5 mg/kg	$t_{1/2}$ (h)	0.4
Solubility (μM)[c]	JP-1 (pH = 1.2)	>100		Clearance (mL/min/kg)	53
	JP-2 (pH = 6.8)	<0.5		Vd (L/kg)	1.3
Stability (%)[d]	MLM	51	(po) 20 mg/kg	C_{max} (μg/mL)	2.9
	HLM	65		T_{max} (h)	1.3
				$AUC_{(0\ to\ 8\ h)}$ (μg h/mL)	6.8
CYP Inhibition IC_{50} (μM)	1A2	18	*F* (%)		>95
	2C9	3.0			
	2C19	14			
	2D6	27			
	3A4	1.6			

[a] Values are the arithmetic means of at least two experiments.
[b] The *c* log *P* values were calculated by CLOGP software (Version 4.8.2, Daylight Chemical Information Systems, Inc.).
[c] Aqueous acidic (JP-1) and neutral solution (JP-2) were purchased from Kanto Chemical Co., Inc. The sample solution was assayed using HPLC methodologies. 250 μM of the compound solution in aqueous CH_3CN solution (1:1 (v/v)) was prepared to make a calibration curve. The solubility was determined by comparing the UV peak area of the standard solution.
[d] Stability is described as % remaining after 30 min incubation with murine liver microsomes (MLM) or human liver microsomes (HLM).
[e] A dose of each compound was either intravenously (5 mg/kg, DMA/Tween80/saline = 10:10:80) injected into the tail vein of C57BL/6J mice ($n = 2$) or orally (20 mg/kg, PG/Tween = 4:1, $n = 3$) administered using an intubation tube. Plasma samples (20 μL) were collected up to 8 h after intravenous or oral administration.

substituted spiropiperidines. The 5-CF_3 (**10c**) and 5-F (**10e**) substituted analogs demonstrated higher C_{max} and AUC than other congeners. The high plasma exposure of the two compounds clearly explains their higher potency in the liver desaturase inhibition in db/db mice as shown in Table 2. These ADME and PK properties further establish **10e** as a solid alternative to **10c**.

The ADME and PK properties of **10e** were further evaluated and are summarized in Table 4. **10e** showed modest metabolic stability in the presence of murine or human liver microsomes (MLM, HLM), explaining the relatively rapid clearance (53 mL/min/kg) and short plasma half-life ($t_{1/2} = 0.4$ h) after intravenous administration to C57BL/6J mice. Oral bioavailability is favorably high (>95%), indicating that **10e** is readily absorbed after oral administration to C57BL/6J mice. As for CYP inhibition, **10e** showed marginal inhibitory activity with IC_{50} values over 10 μM against CYP1A2, 2C9, and 2D6, and a somewhat higher potency for the inhibition of 2C9 and 3A4. Although CYP3A4 inhibition is a concern, the selectivity for human SCD1 is sufficiently high (>5000 fold).

For the analysis of the in vivo efficacy of SCD1 inhibitors, we took note that Attie and co-workers reported that the hepatic triglyceride levels of mice on a very low-fat diet increased by 240% [36,37]. We assumed that the SCD1 activity in the liver of these mice was very high and we were interested in the inhibitory effect of the spiropiperidine-based SCD1 inhibitors against the liver SCD1 in C57BL/6J mice on a high carbohydrate diet, which was composed of protein (22.2 kcal%) and carbohydrates (77.8 kcal%). **10e** was tested in a 7-day efficacy study using C57BL/6J mice on a high carbohydrate diet. The desaturation index, calculated as the ratio of C18:1/C18:0, was used as an in vivo biomarker. After once-daily administration for 7 days, **10e** dose-dependently reduced the plasma desaturation index with a 32% reduction at 0.3 mg/kg and 66% reduction at 10 mg/kg (Fig. 3). The

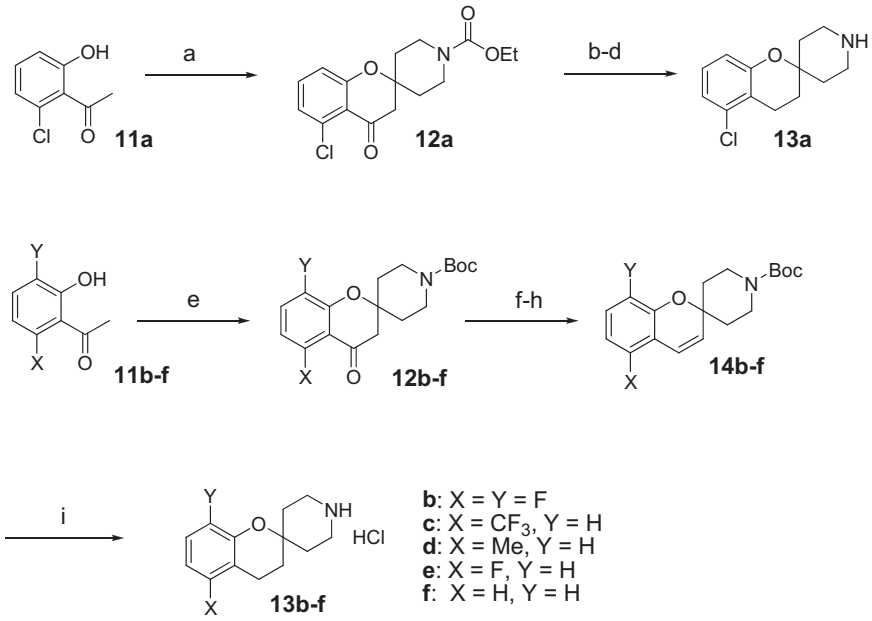

Scheme 1. Synthesis of properly substituted spiropiperidines. Reagents and Conditions: (a) pyrrolidine, ethyl 4-oxopiperidine-1-carboxylate, EtOH, 0 °C to rt, 34%; (b) NaBH4, MeOH/THF, rt, 68%; (c) Et3SiH, $BF_3 \cdot Et_2O$, CH_2Cl_2, rt to 40 °C, 95%; (d) KOH, EtOH/H_2O, reflux; 95%; (e) tert-butyl 4-oxopiperidine-1-carboxylate, pyrrolidine, PrOH or EtOH, 0 °C ~ reflux; (f) $NaBH_4$, MeOH, rt; (g) MsCl, Et_3N, CH_2Cl_2; (h) DBU, NMP, 100 °C; (i) Pd/C (10wt%), H_2, 1 N HCl (If necessary, acidic deprotection (4 N HCl, 1,4-dioxane) was followed).

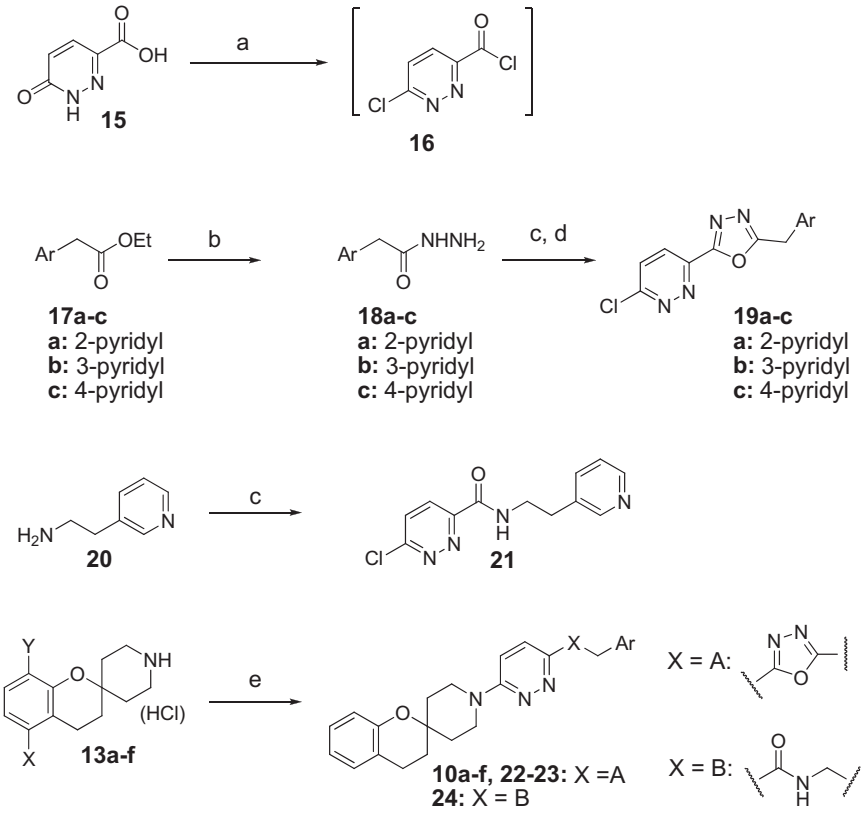

Scheme 2. The preparation of the chloropyridazine intermediates and the final condensation. Reagents and Conditions: (a) $SOCl_2$, DMF, $CHCl_3$, 50∼55 °C; (b) hydrazine monohydrate, EtOH, quantitative yield; (c) 16, Et_3N, DMF; (d) TsCl, DMAP, CH_3CN; (e) 19 (or 21), Et_3N, n-BuOH, 100 °C.

reduction of the desaturation index at 1 mg/kg was even greater than that observed in mice on a normal diet (FR-2), indicating the substantial power of **10e** in exerting inhibitory activity against SCD1 in the tested mice. As for the safety issue, our attention was mainly focused on the skin and eyes of the tested mice because cutaneous abnormalities and narrow eye fissure have been reported in studies on SCD1-deficient mice [38,39]. We did not observe abnormalities in the skin of the C57BL/6J mice at10 mg/kg during the period of dosing. While mild eye fissure was observed in C57BL/6J mice at 3 and 10 mg/kg, analysis of the tissue around the eyes of the tested mice revealed that there was not any notable change in the size and color of Harderian gland, where SCD is reported to be highly expressed [40]. In the autopsy of the C57BL/6J mice after the 7-day treatment with **10e**, notable changes were not observed in the organs up to 10 mg/kg. We assume that the balanced combination of the strong potency and short plasma half-life of **10e** resulted in pharmacological efficacy in vivo and may be beneficial in preventing severe adverse events. While this is a preliminary speculation, the relatively short plasma half-life of **10e** may help to accomplish favorable tissue selectivity (liver over skin). Currently, we do not know the long term toxicological effect of **10e**. However, more distinct abnormalities [38,39] may be observable with an extended administration period.

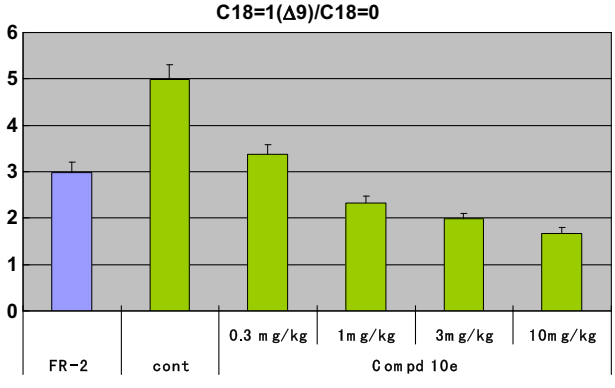

Fig. 3. Plasma desaturation index lowering effect of **10e** after 7 days (q.d.) in C57BL/6J mice ($n = 4$) fed a high carbohydrate diet.

4. Conclusion

As an extension of our continuing efforts in the investigation of novel treatments for metabolic disorders, this article describes the synthesis, SAR, PK properties, and pharmacological evaluation of the novel SCD1 inhibitors. Preparation of a series of the spiropiperidine-based SCD1 inhibitors and careful SAR analysis confirmed the importance of the 3-pyridyl group in the right side part for strong inhibitory activity against the liver desaturase in db/db mice. The SAR analysis also showed that the 1,3,4-oxadiazole ring was an effective replacement for amide bond. PK analysis of the highly potent SCD1 inhibitors (**10a**–**f**) revealed that specific substitution in the 5-position of the spiropiperidine was necessary for better plasma exposure in mice. The current investigation finally led us to identify a highly potent SCD1 inhibitor: 5-fluoro-1′-{6-[5-(pyridin-3-ylmethyl)-1,3,4-oxadiazol-2-yl]pyridazin-3-yl}-3,4-dihydrospiro[chromene-2,4′-piperidine] (**10e**), which demonstrated a very strong potency in liver SCD1 inhibition ($ID_{50} = 0.6$ mg/kg). This highly efficacious inhibition is presumed to be a result of a combination of

strong enzymatic inhibitory activity (IC_{50} (mouse) = 2 nM) and good oral bioavailability (F >95%). Easier synthetic accessibility of **10e** has turned it to an attractive alternative to **10c**, which was previously reported as a highly potent SCD1 inhibitor. With regard to the pharmacological evaluation, **10e** demonstrated striking reduction of the desaturation index in a dose-dependent manner in the plasma of C57BL/6J mice on a high carbohydrate diet after a 7-day oral administration (q.d.). In addition, it did not cause noticeable abnormalities in the skin up to the highest dose (10 mg/kg). Further pharmacological evaluation and toxicological analysis of the spiropiperidine-based SCD1 inhibitors will be reported in the future.

5. Experimental

5.1. Chemistry

5.1.1. General procedures

All melting points were measured with a Mettler Toledo Thermo System FP8HT and are uncorrected. The IR spectra were measured with a JEOL FT/IR 6100 spectrophotometer, and the peaks were recorded in cm^{-1}. ^1H NMR spectra were recorded on a Varian Mercury 400 or 500 spectrometer with tetramethylsilane as an internal reference. The mass spectra (low- or high-resolution mass) spectroscopy was carried out with a JEOL GCmate, JEOL JMS-700 mass spectrometer or JEOL T100LC (AccuTOF). Thin-layer chromatography (TLC) was used routinely to monitor the progress and the purity of the compounds and was performed on Merck Kieselgel 60 F_{254} plates (0.25 mm thickness). For the flash column chromatography, silica gel (Kieselgel 60, 230–400 mesh) or pre-packed silica gel column (KP-Sil™ silica) from Biotage was employed. The *o*-hydroxyacetophenones (**11e**–**f**) were commercially available. The experimental procedures for the preparation of the intermediates in Schemes 1 and 2 are described in Supplementary data.

5.1.2. General synthetic procedures to obtain spiropiperidine-based SCD1 inhibitor (*10a–f*, *22–24*) from spiropiperidine (*13a–f*) and chloropyridazine (*19a–c*, *21*)

A mixture of spiropiperidine (**13**, 1 equiv), chloropyridazine (**19** or **21**, 1 equiv), and triethylamine (2 equiv) in n-BuOH was heated at 100 °C for 2 days, cooled to room temperature, and concentrated. Chromatography of the residue on SiO_2 (Chromatorex NH Fuji Silysia Chemical Ltd. 200–300 mesh, CH_2Cl_2/EtOAc 1:0 to 3:1) gave the desired product (**10**, **22**, **23**, or **24**). The product was further purified by recrystallization when necessary.

5.1.2.1. 5-Chloro-1′-{6-[5-(pyridin-3-ylmethyl)-1,3,4-oxadiazol-2-yl]pyridazin-3-yl}-3,4-dihydrospiro[chromene-2,4′-piperidine] (*10a*).

In accordance with the general procedures (Section 5.1.2), **13a** (29.2 mg, 0.123 mmol) and **19b** (28.0 mg, 0.102 mmol) provided 31.0 mg of **10a** (64%) as a yellow amorphous. ^1H NMR (500 MHz, DMSO-d_6): δ 8.64 (1H, d, J = 2.0 Hz), 8.53 (1H, dd, J = 4.3 and 1.4 Hz), 7.97 (1H, d, J = 9.8 Hz), 7.82 (1H, d, J = 7.8 Hz), 7.45 (1H, d, J = 9.7 Hz), 7.42 (1H, dd, J = 7.8 and 4.8 Hz), 7.14 (1H, t, J = 8.0 Hz), 7.00 (1H, d, J = 7.8 Hz), 6.85 (1H, d, J = 7.3 Hz), 4.46 (2H, s), 4.29–4.24 (2H, m), 3.52–3.45 (2H, m), 2.73 (2H, t, J = 6.6 Hz), 1.89 (2H, t, J = 6.8 Hz), 1.85–1.80 (2H, m), 1.74–1.68 (2H, m). IR (KBr, cm^{-1}): 3064, 2953, 2846, 1595, 1446, 1430, 1248. MS (ESI) m/z: 475 $(M+H)^+$; HRMS (ESI) m/z: 475.1646 (calcd for $C_{25}H_{24}ClN_6O_2$ 475.1649). Anal. Calcd for $C_{25}H_{23}ClN_6O_2$: C, 63.22; H, 4.88; N, 17.69; Cl, 7.46. Found: C, 63.08; H, 4.83; N, 17.55; Cl, 7.47.

5.1.2.2. 5,8-Difluoro-1′-{6-[5-(pyridin-3-ylmethyl)-1,3,4-oxadiazol-2-yl]pyridazin-3-yl}-3,4-dihydrospiro[chromene-2,4′-piperidine] (*10b*).

In accordance with the general procedures (Section 5.1.2), **13b** (97.2 mg, 0.353 mmol) and **19b** (93.7 mg, 0.342 mmol) provided 84.8 mg of **10b** (52%) as a colorless solid. Mp 192–193 °C. ^1H NMR (400 MHz, $CDCl_3$): δ 8.67 (1H, d, J = 2.0 Hz), 8.57 (1H, dd, J = 4.7 and 1.6 Hz), 8.03 (1H, d, J = 9.4 Hz), 7.77 (1H, d, J = 7.8 Hz), 7.30 (1H, dd, J = 8.1 and 4.9 Hz), 7.02 (1H, d, J = 9.8 Hz), 6.93–6.87 (1H, m), 6.57–6.52 (1H, m), 4.41–4.38(2H, m), 4.33 (2H, s), 3.63–3.55 (2H, m), 2.79 (2H, t, J = 6.9 Hz), 2.03–2.00 (2H, m), 1.87 (2H, t, J = 6.9 Hz), 1.76–1.68 (2H, m). IR (KBr, cm^{-1}): 3067, 2926, 2859, 1592, 1488, 1447, 1262, 1236. MS (ESI) m/z: 477$(M+H)^+$; HRMS (ESI) m/z: 477.1852 (calcd for $C_{25}H_{23}F_2N_6O_2$ 477.1851). Anal. Calcd for $C_{25}H_{22}F_2N_6O_2$: C, 63.02; H, 4.65; N, 17.64; F, 7.97. Found: C, 62.86; H, 4.66; N, 17.48; F, 8.04.

5.1.2.3. 1′-{6-[5-(Pyridin-3-ylmethyl)-1,3,4-oxadiazol-2-yl]pyridazin-3-yl}-5-(trifluoromethyl)-3,4-dihydrospiro[chromene-2,4′-piperidine] (*10c*).

In accordance with the general procedures (Section 5.1.2), **13c** (554 mg, 1.80 mmol) and **19b** (465 mg, 1.70 mmol) provided 587 mg (68%) of **10c** as a white solid. Mp 217–218 °C (*i*PrOH). ^1H NMR (400 MHz, DMSO-d_6): δ 8.65 (1H, d, J = 2.4 Hz), 8.54 (1H, dd, J = 4.7 and 1.5 Hz), 7.99 (1H, d, J = 9.8 Hz), 7.84 (1H, d, J = 7.8 Hz), 7.47 (1H, d, J = 9.8 Hz), 7.43 (1H, dd, J = 7.8 and 4.7 Hz), 7.33 (1H, t, J = 8.0 Hz), 7.27 (1H, d, J = 6.7 Hz), 7.17 (1H, d, J = 8.3 Hz), 4.47 (2H, s), 4.30–4.26 (2H, m), 3.54–3.48 (2H, m), 2.89 (2H, t, J = 6.6 Hz), 1.91 (2H, t, J = 6.6 Hz), 1.86–1.83 (2H, m), 1.77–1.70 (2H, m). IR (KBr, cm^{-1}): 3065, 2958, 2851, 1594, 1463, 1431, 1320, 1258. MS (ESI) m/z: 509 $(M+H)^+$; HRMS (ESI) m/z: 509.1915 (calcd for $C_{26}H_{24}F_3N_6O_2$ 509.1913). Anal. Calcd for $C_{26}H_{23}F_3N_6O_2$: C, 61.41; H, 4.56; N, 16.53; F, 11.21. Found: C, 61.33; H, 4.62; N, 16.45; F, 11.37.

5.1.2.4. 5-Methyl-1′-{6-[5-(pyridin-3-ylmethyl)-1,3,4-oxadiazol-2-yl]pyridazin-3-yl}-3,4-dihydrospiro[chromene-2,4′-piperidine] (*10d*).

In accordance with the general procedures (Section 5.1.2), **13d** (254 mg, 1.00 mmol) and **19b** (274 mg, 1.00 mmol) provided 387 mg of **10d** (58%) as a white solid. Mp 194–195 °C. ^1H NMR (400 MHz, DMSO-d_6): δ 8.63 (1H, s), 8.52 (1H, d, J = 4.7 Hz), 7.95 (1H, d, J = 9.4 Hz), 7.83–7.80 (1H, m), 7.43 (1H, d, J = 9.7 Hz), 7.41–7.39 (1H, m), 6.97 (1H, dd, J = 7.6 and 7.6 Hz), 6.71 (1H, d, J = 7.0 Hz), 6.66 (1H, d, J = 8.2 Hz), 4.45(2H, s), 4.28–4.21 (2H, m), 3.49–3.43 (2H, m), 2.60 (2H, t, J = 6.9 Hz), 2.17 (3H, s), 1.83 (2H, t, J = 6.9 Hz), 1.82–1.78 (2H, m), 1.69–1.62 (2H, m). IR (KBr, cm^{-1}): 3068, 2953, 2924, 2847, 1594, 1536, 1466, 1429, 1250; MS (ESI) m/z: 455 $(M+H)^+$; HRMS (ESI) m/z: 455.2189 (calcd for $C_{26}H_{27}N_6O_2$ 455.2196). Anal. Calcd for $C_{25}H_{22}F_2N_6O_2$: C, 68.70; H, 5.77; N, 18.49. Found: C, 68.42; H, 5.75; N, 18.42.

5.1.2.5. 5-Fluoro-1′-{6-[5-(pyridin-3-ylmethyl)-1,3,4-oxadiazol-2-yl]pyridazin-3-yl}-3,4-dihydrospiro[chromene-2,4′-piperidine] (*10e*).

In accordance with the general procedures (Section 5.1.2), **13e** (541 mg, 2.11 mmol) and **19b** (547 mg, 2.00 mmol) provided 682 mg of **10e** (74%) as a pale pink solid. Mp 183–185 °C (CH_3CN/iPr_2O). ^1H NMR (400 MHz, DMSO-d_6): δ 8.65 (1H, d, J = 2.0 Hz), 8.54 (1H, dd, J = 4.9 and 1.3 Hz), 7.99 (1H, d, J = 9.8 Hz), 7.84 (1H, d, J = 7.9 Hz), 7.47 (1H, d, J = 9.3 Hz), 7.43 (1H, dd, J = 7.7 and 4.9 Hz), 7.14 (1H, dd, J = 15.3 and 7.8 Hz), 6.73–6.69 (2H, m), 4.47 (2H, s), 4.30–4.20 (2H, m), 3.52–3.42 (2H, m), 2.71 (2H, t, J = 6.4 Hz), 1.87(2H, t, J = 7.0 Hz), 1.87–1.83 (2H, m), 1.75–1.68 (2H, m). IR (KBr, cm^{-1}): 3057, 2948, 2866, 1593, 1467, 1446, 1254. MS (ESI) m/z: 459 $(M+H)^+$; HRMS (ESI) m/z: 459.1936 (calcd for $C_{25}H_{24}FN_6O_2$ 459.1945). Anal. Calcd for $C_{25}H_{23}FN_6O_2$: C, 65.49; H, 5.06; N, 18.33; F, 4.14. Found: C, 65.31; H, 5.12; N, 18.23; F, 4.02.

5.1.2.6. 1′-{6-[5-(Pyridin-3-ylmethyl)-1,3,4-oxadiazol-2-yl]pyridazin-3-yl}-3,4-dihydrospiro[chromene-2,4′-piperidine] (*10f*).

In accordance with the general procedures (Section 5.1.2), **13f** (791 mg,

3.30 mmol) and **19b** (821 mg, 3.00 mmol) provided 1.14 g of **10f** (86%) as a pink solid. Mp 176–177 °C. ^{1}H NMR (400 MHz, DMSO-d_6): δ 8.62 (1H, d, J = 1.1 Hz), 8.51 (1H, d, J = 4.7 Hz), 7.96 (1H, d, J = 9.8 Hz), 7.81 (1H, d, J = 7.8 Hz), 7.44 (1H, d, J = 10.5 Hz), 7.41 (1H, dd, J = 8.2 and 5.5 Hz), 7.07 (2H, t, J = 7.4 Hz), 6.81 (2H, t, J = 7.6 Hz), 4.45 (2H, s), 4.27–4.24(2H, m), 3.51–3.45 (2H, m), 2.74 (2H, t, J = 6.9 Hz), 1.83–1.80 (2H, m), 1.81 (2H, t, J = 6.4 Hz), 1.71–1.64 (2H, m). IR (KBr, cm^{-1}): 3053, 2920, 2868, 1595, 1540, 1486, 1453, 1226. MS (ESI) m/z: 441 $(M+H)^+$; HRMS (ESI) m/z: 441.2041 (calcd for $C_{25}H_{25}N_6O_2$ 441.2039). Anal. Calcd for $C_{25}H_{24}N_6O_2$: C, 68.17; H, 5.49; N, 19.08. Found: C, 67.85; H, 5.51; N, 18.90.

*5.1.2.7. 1′-{6-[5-(Pyridin-2-ylmethyl)-1,3,4-oxadiazol-2-yl]pyridazin-3-yl}-3,4-dihydrospiro[chromene-2,4′-piperidine] (**22**).* In accordance with the general procedures (Section 5.1.2), **13f** (119 mg, 0.500 mmol) and **19a** (106 mg, 0.450 mmol) provided 134 mg of **22** (68%) as a pale brown solid. Mp 153–154 °C. ^{1}H NMR (400 MHz, DMSO-d_6): δ 8.49 (1H, d, J = 5.1 Hz), 7.96 (1H, d, J = 9.7 Hz), 7.84–7.79 (1H, m), 7.48 (1H, d, J = 7.8 Hz), 7.43 (1H, d, J = 9.8 Hz), 7.32 (1H, dd, J = 7.4 and 4.7 Hz), 7.07 (2H, t, J = 7.2 Hz), 6.81 (2H, t, J = 7.4 Hz), 4.55 (2H, s), 4.26–4.23 (2H, m), 3.50–3.43 (2H, m), 2.73 (2H, t, J = 6.6 Hz), 1.82–1.79 (2H, m), 1.80 (2H, t, J = 6.7 Hz), 1.70–1.63 (2H, m). IR (KBr, cm^{-1}): 3054, 2952, 2866, 1593, 1539, 1229. MS (ESI) m/z: 441 $(M+H)^+$; HRMS (ESI) m/z: 441.2037 (calcd for $C_{25}H_{25}N_6O_2$ 441.2039). Anal. Calcd for $C_{25}H_{24}N_6O_2$: C, 68.17; H, 5.49; N, 19.08. Found: C, 68.08; H, 5.61; N, 18.80.

*5.1.2.8. 1′-{6-[5-(Pyridin-4-ylmethyl)-1,3,4-oxadiazol-2-yl]pyridazin-3-yl}-3,4-dihydrospiro[chromene-2,4′-piperidine] (**23**).* In accordance with the general procedures (Section 5.1.2), **13f** (59.9 mg, 0.250 mmol) and **19c** (62.6 mg, 0.228 mmol) provided 86.5 mg of **23** (87%) as a yellow amorphous. ^{1}H NMR (400 MHz, DMSO-d_6): δ 8.57 (2H, m), 7.98 (1H, d, J = 9.8 Hz), 7.46 (1H, d, J = 9.8 Hz), 7.42 (2H, d, J = 5.9 Hz), 7.09 (2H, t, J = 7.4 Hz), 6.83 (2H, t, J = 7.4 Hz), 4.48 (2H, s), 4.29–4.26 (2H, m), 3.53–3.46 (2H, m), 2.76 (2H, t, J = 6.6 Hz), 1.85–1.81 (2H, m), 1.83 (2H, t, J = 6.4 Hz), 1.73–1.65(2H, m). IR (KBr, cm^{-1}): 3026, 2943, 2851, 1596, 1542, 1487, 1449, 1230. MS (ESI) m/z: 441 $(M+H)^+$; HRMS (ESI) m/z: 441.2031 (calcd for $C_{25}H_{25}N_6O_2$ 441.2039). Anal. Calcd for $C_{25}H_{24}N_6O_2$: C, 68.17; H, 5.49; N, 19.08. Found: C, 67.56; H, 5.42; N, 18.65.

*5.1.2.9. 6-(3,4-Dihydro-1′H-spiro[chromene-2,4′-piperidin]-1′-yl)-N-(2-pyridin-3-ylethyl)pyridazine-3-carboxamide (**24**).* In accordance with the general procedures (Section 5.1.2), **13f** (839 mg, 3.50 mmol) and **21** (866 mg, 3.30 mmol) provided 1.40 g of **24** (98%) as pale brown solid. Mp 152–154 °C. ^{1}H NMR (400 MHz, DMSO-d_6): δ 8.90–8.88 (1H, m), 8.43 (1H, s), 8.39 (1H, d, J = 4.7 Hz), 7.79 (1H, d, J = 8.2 Hz), 7.65 (1H, d, J = 7.9 Hz), 7.37 (1H, d, J = 9.8 Hz), 7.29 (1H, dd, J = 7.8 and 4.6 Hz), 7.09–7.05 (2H, m), 6.83–6.79 (2H, m), 4.24–4.20 (2H, m), 3.58–3.53(2H, m), 3.49–3.42 (2H, m), 2.88 (2H, t, J = 6.9 Hz), 2.74 (2H, t, J = 6.5 Hz), 1.82–1.78 (2H, m), 1.81(2H, t, J = 6.9 Hz), 1.70–1.63 (2H, m). IR (KBr, cm^{-1}): 3420, 2948, 2866, 1668, 1588, 1514, 1486, 1445, 1227. MS (ESI) m/z: 430 $(M+H)^+$; HRMS (ESI) m/z: 430.2244 (calcd for $C_{25}H_{28}N_5O_2$ 430.2243). Anal. Calcd for $C_{25}H_{27}N_5O_2$: C, 69.91; H, 6.34; N, 16.31. Found: C, 69.52; H, 6.40; N, 16.19.

5.2. Biology

5.2.1. Desaturase enzymatic assay

The SCD1 activity was determined by measuring the conversion of stearate to oleate. In each reaction tube, test compounds were preincubated with 10 μL microsomes for 10 min at room temperature. The SCD1 reaction was started by the addition of 40 μL of a mixture containing 250 mM sucrose, 150 mM KCl, 40 mM NaF, 5 mM $MgCl_2$, 100 mM sodium phosphate, pH7.4, 1 mM ATP, 1.5 mM reduced glutathione, 0.06 mM reduced coenzyme A, 0.33 mM nicotinamide, 1.25 mM NADH and 0.01 μCi [^{14}C] stearate. After 60 min incubation at 37 °C, the reaction was stopped by adding 50 μL methanol containing 10% KOH and then the mixture was saponified at 80 °C for 30 min. The free fatty acids in the reaction were protonated by the addition of 5 N HCl (15 μL) and extracted with 100 μL ethyl acetate. Thirty microlitres of the ethyl acetate extracts of each reaction was charged to an $AgNO_3$-TLC plate (20 × 20 cm LK5D plates, 150+ pore diameter, 250 μm thick) and differentiated in a solvent consisting of chloroform/methanol/acetate/water (90:8:1:0.8). [^{14}C] stearate and [^{14}C] oleate were quantified with BAS2500 (Fujifilm) and SCD1 activity was determined as the ratio of [^{14}C] oleate to [^{14}C] stearate. The IC_{50} values were calculated by linear regression using the straight line portions of the concentration–response curve. To measure the delta-6 desaturase activity, [^{14}C] linolenic acid was used as the substrate and the delta-6 desaturase activity was determined as the ratio of [^{14}C] C18:3 $n-3$ to [^{14}C] C18:4 $n-3$.

5.2.2. Cellular assay

A 293A cell-based desaturase assay was performed in a 96-well plate. Human SCD1 gene was cloned into the expression vector pCMV-script (Stratagene). 293A cells were transfected with the expression vector. The cells stably expressing human SCD1 were selected with G418. The 293A cells in 100 μL media (DMEM + 10% FBS) were seeded to each well of a 96-well plate and grown overnight to be confluent. The cells were preincubated with the test compound in fresh media for 30 min, after which 10 μL media containing 0.1 μCi [^{14}C] stearate was added to each well and incubated for another 4 h. Then the cells in each well were washed with cold PBS and the cellular lipids were saponified directly by adding 100 μL of 5% KOH in methanol/H_2O (1:1). The samples were processed as described for the SCD1 enzymatic assay to determine the SCD1 activity by quantifying the ratio of [^{14}C] oleate to [^{14}C] stearate.

5.2.3. Determination of ID_{50} (db/db mice)

SCD1 inhibitors were administered to 7-week-old db/db male mice by oral gavage 2 h prior to the administration of [^{14}C] stearate. Then the mice were injected i.p. with 5 mL/kg of 20 μCi/mL [^{14}C] stearate solution in saline containing 2% BSA, resulting in a bolus amount of 100 μCi/kg. One hour after the injection of [^{14}C] stearate, the mice were sacrificed and their livers were removed and quickly frozen in liquid nitrogen. The livers were homogenized in 9× volume of cold PBS, and 250 μL of homogenate was mixed with an equal volume of methanol containing 10% KOH. Then the samples were processed as described for the SCD1 enzymatic assay to determine the SCD1 activity by quantifying the ratio of [^{14}C] oleate to [^{14}C] stearate. The dose at which 50% of SCD1 activity was inhibited is described as ID_{50}.

5.2.4. Desaturation index

Nine-week-old male C57BL6J mice grown with a normal chow diet were fed with a high carbohydrate diet (Research Diets, Inc., D05052506) for 7 days [This diet is composed of protein (22.2 kcal%) and carbohydrates (77.8 kcal%).].

Compound **10e** was administered daily at doses of 0.3, 1, 3 and 10 mg/kg to male C57BL6J mice on a high carbohydrate diet for 7 days in the evening by oral gavage in propylene glycol/Tween 80 (4/1) formulation (dosing vehicle). The animals were allowed free access to the high carbohydrate diet and water throughout the study. After the seventh dose, the animals were sacrificed in the morning and the blood serum was assayed for the desaturation index as follows. Thirty microlitres serum was mixed with 4 mL 0.5 N KOH in methanol and saponified at 100 °C for 30 min. The free fatty acids in

the reaction were protonated by the addition of 2 mL of 1 N HCl and extracted with 3 mL of n-hexane. Two mL of the hexane extracts was dried up, dissolved with 1 mL of BF_3/methanol, and then was esterified at 100 °C for 15 min. The samples were mixed with 1 mL of H_2O and extracted with 1 mL n-hexane. One microlitre of the final hexane extracts was loaded to a gas chromatogram to determine the stearate and oleate content. The desaturation index was calculated as the ratio of oleate to stearate.

Appendix. Supplementary data

Supplementary data associated with this article can be found in the online version, at doi:10.1016/j.ejmech.2010.07.044.

References

[1] J.M. Ntambi, Prog. Lipid Res. 34 (1995) 139–150.
[2] A. Dobrzyn, J.M. Ntambi, Obes. Rev. 6 (2005) 169–174.
[3] J.M. Ntambi, M. Miyazaki, Curr. Opin. Lipidol. 14 (2003) 255–261.
[4] M. Miyazaki, M.J. Jacobsen, W.C. Man, P. Cohen, E. Asilmaz, J.M. Friedman, J.M. Ntambi, J. Biol. Chem. 278 (2003) 33904–33911.
[5] J. Wang, L. Yu, R.E. Schmidt, C. Su, X. Huang, K. Gould, G. Cao, Biochem. Biophys. Res. Commun. 332 (2005) 735–742.
[6] L. Zhang, L. Ge, S. Parimoo, K. Stenn, S.M. Prouty, Biochem. J. 340 (1999) 255–264.
[7] M. Miyazaki, C. Y-Kim, M.P. Gray-Keller, A.D. Attie, J.M. Ntambi, J. Biol. Chem. 275 (2000) 30132–30138.
[8] M.T. Flowers, J.M. Ntambi, Curr. Opin. Lipidol. 19 (2008) 248–256.
[9] M. Miyazaki, H. Sampath, X. Liu, M.T. Flowers, K. Chu, A. Dobrzyn, J.M. Ntambi, Biochem. Biophys. Res. Commun. 380 (2009) 818–822.
[10] P. Dobrzyn, A. Dobrzyn, Drug Dev. Res. 67 (2006) 643–650.
[11] A.D. Attie, R.M. Krauss, M.P. Gray-Keller, A. Brownlie, M. Miyazaki, J.J. Kastelein, A.J. Lusis, A.F.H. Stalenhoef, J.P. Stoehr, M.R. Hayden, J.M. Ntambi, J. Lipid Res. 43 (2002) 1899–1907.
[12] A. Peter, A. Cegan, S. Wagner, R. Lehmann, N. Stefan, A. Königsrainer, I. Königsrainer, H.-U. Häring, E. Schleicher, Clin. Chem. 55 (2009) 2113–2120.
[13] For the typical structures of Xenon's SCD1 inhibitors, see: M. Abreo, M. Chafeev, N. Chakka, S. Chowdhury, J.-M. Fu, H.W. Gschwend, M.W. Holladay, D. Hou, R. Kamboj, V. Kodumuru, W. Li, S. Liu, V. Raina, S. Sun, S. Sun, S. Sviridov, C. Tu, M.D. Winther, Z. Zhang, WO2005011655A2, Feb. 10, 2005.
[14] For patent applications describing SCD1 inhibitors, see: G. Liu Expert. Opin. Ther. Patents 19 (2009) 1169–1191.
[15] G. Liu, Curr. Top. Med. Chem. 10 (2010) 419–433.
[16] C.S. Li, L. Belair, J. Guay, R. Murgasva, W. Sturkenboom, Y.K. Ramtohul, L. Zhang, Z. Huang, Bioorg. Med. Chem. Lett. 19 (2009) 5214–5217.
[17] S. Léger, W.C. Black, D. Deschenes, S. Dolman, P. J-Falgueyret, M. Gagnon, S. Guiral, Z. Huang, J. Guay, Y. Leblanc, C.S. Li, F. Massé, R. Oballa, L. Zhang, Bioorg. Med. Chem. Lett. 20 (2010) 499–502.
[18] Y.K. Ramtohul, C. Black, C.-C. Chan, S. Crane, J. Guay, S. Guiral, Z. Huang, R. Oballa, J. L-Xu, L. Zhang, C.S. Li, Bioorg. Med. Chem. Lett. 20 (2010) 1593–1597.
[19] G. Liu, J.K. Lynch, J. Freeman, B. Liu, Z. Xin, H. Zhao, M.D. Serby, P.R. Kym, T.S. Suhar, H.T. Smith, N. Cao, R. Yang, R.S. Janis, J.A. Krauser, S.P. Cepa, D.W.A. Beno, H.L. Sham, C.A. Collins, T.K. Surowy, H.S. Camp, J. Med. Chem. 50 (2007) 3086–3100.
[20] H. Zhao, M.D. Serby, H.T. Smith, N. Cao, T.S. Suhar, T.K. Surowy, H.S. Camp, C.A. Collins, H.L. Sham, G. Li, Bioorg. Med. Chem. Lett. 17 (2007) 3388–3391.
[21] Z. Xin, H. Zhao, M.D. Serby, B. Liu, M. Liu, B.G. Szczepankiewicz, L.T.J. Nelson, H.T. Smith, T.S. Suhar, R.S. Janis, N. Cao, H.S. Camp, C.A. Collins, H.L. Sham, T.K. Surowy, G. Li, Bioorg. Med. Chem. Lett. 18 (2008) 4298–4302.
[22] D.O. Koltun, E.Q. Parkhill, N.I. Vasilevich, A.I. Glushkov, T.M. Zilbershtein, A.V. Ivanov, A.G. Cole, I. Henderson, N.A. Zautke, S.A. Brunn, N. Mollova, K. Leung, J.W. Chisholm, J. Zablocki, Bioorg. Med. Chem. Lett. 19 (2009) 2048–2052.
[23] D.O. Koltun, N.I. Vasilevich, E.Q. Parkhill, A.I. Glushkov, T.M. Zilbershtein, E.I. Mayboroda, M.A. Boze, A.G. Cole, I. Henderson, N.A. Zautke, S.A. Brunn, N. Chu, J. Hao, N. Mollova, K. Leung, J.W. Chisholm, J. Zablocki, Bioorg. Med. Chem. Lett. 19 (2009) 3050–3053.
[24] D.O. Koltun, T.M. Zilbershtein, V.A. Migulin, N.I. Vasilevich, E.Q. Parkhill, A.I. Glushkov, M.J. McGregor, S.A. Brunn, N. Chu, J. Hao, N. Mollova, K. Leung, J.W. Chisholm, J. Zablocki, Bioorg. Med. Chem. Lett. 19 (2009) 4070–4074.
[25] H. Yamaguchi, N. Sawada, M. Hashizume, T. Kamei, F. Hasegawa, T. Mimoto, in: 27th Med. Chem. Symp., Abst. 1P-57, November 26–28 2008, Osaka, Japan.
[26] M. Issandou, A. Bouillot, J.-M. Brusq, M.-C. Forest, D. Grillot, R. Guillard, S. Martin, C. Michiels, T. Sulpice, A. Daugan, Eur. J. Pharmacol. 618 (2009) 28–36.
[27] Y. Uto, T. Ogata, J. Harada, Y. Kiyotsuka, Y. Ueno, Y. Miyazawa, H. Kurata, T. Deguchi, N. Watanabe, T. Takagi, S. Wakimoto, R. Okuyama, M. Abe, N. Kurikawa, S. Kawamura, M. Yamato, J. Ohsumi, Bioorg. Med. Chem. Lett. 19 (2009) 4151–4158.
[28] Y. Uto, T. Ogata, Y. Kiyotsuka, Y. Miyazawa, Y. Ueno, H. Kurata, T. Deguchi, M. Yamada, N. Watanabe, T. Takagi, S. Wakimoto, R. Okuyama, M. Konishi, N. Kurikawa, K. Kono, J. Ohsumi, Bioorg. Med. Chem. Lett. 19 (2009) 4159–4167.
[29] Y. Uto, T. Ogata, Y. Kiyotsuka, Y. Ueno, Y. Miyazawa, H. Kurata, T. Deguchi, N. Watanabe, M. Konishi, R. Okuyama, N. Kurikawa, T. Takagi, S. Wakimoto, J. Ohsumi, Bioorg. Med. Chem. Lett. 20 (2010) 341–345.
[30] Y. Uto, Y. Kiyotsuka, Y. Ueno, Y. Miyazawa, H. Kurata, T. Ogata, T. Deguchi, M. Yamada, N. Watanabe, M. Konishi, N. Kurikawa, T. Takagi, S. Wakimoto, K. Kono, J. Ohsumi, Bioorg. Med. Chem. Lett. 20 (2010) 746–754.
[31] D.M. Tschaen, L. Abramson, D. Cai, R. Desmond, H. U-Dolling, L. Frey, S. Karady, Y.-J. Shi, T.R. Verhoeven, J. Org. Chem. 60 (1995) 4324–4330.
[32] H.-J. Kabbe, A. Widdig, Angew. Chem. Int. Edit. 21 (1982) 247–256.
[33] C.A. James, B. Poirier, C. Grisé, A. Martel, E.H. Ruediger, Tetrahedron Lett. 47 (2006) 511–514.
[34] I.R. Baxendale, S.V. Ley, M. Martinelli, Tetrahedron 61 (2005) 5323–5349.
[35] C.A. Lipinski, F. Lombardo, B.W. Dominy, P.J. Feeney, Adv. Drug Delivery Rev. 46 (2001) 3–26.
[36] M.T. Flowers, A.K. Groen, A.T. Oler, M.P. Keller, Y.J. Choi, K.L. Schueler, O.C. Richards, H. Lan, M. Miyazaki, F. Kuipers, C.M. Kendziorski, J.M. Ntambi, A.E. Attie, J. Lipid Res. 47 (2006) 2668–2680.
[37] The association of high carbohydrate diets with high SCD activity was recently reviewed M.T. Flowers, J.M. Ntambi, BBA-Mol. Cell. Biol. L. 1791 (2009) 85–91.
[38] M. Miyazaki, W.C. Man, J.M. Ntambi, J. Nutr. 131 (2001) 2260–2268.
[39] E. Binczek, B. Jenke, B. Holtz, R.H. Gunter, M. Thevis, W. Stoffel, J. Biol. Chem. 388 (2007) 405–418.
[40] M. Miyazaki, Y.-C. Kim, W.C. Man, J.M. Ntambi, Biol. Chem. 276 (2001) 39455–39461.